PCCP

Accepted Manuscript




ROYAL SOCIETY OF CHEMISTRY

www.rsc.org/pccp

Physical Chemistry Chemical Physics
CREATED USING THE RSC LaTeX PCCP ARTICLE TEMPLATE – SEE www.rsc.org/electronicfiles FOR DETAILS
ARTICLE TYPE www. rsc.org/xxxxxx | XXXXXXXX

# A Quantum Biochemistry Investigation for Willardiine Partial Agonism in AMPA Receptors

**José X. Lima Neto, [a] Umberto L. Fulco,*[a] Eudenilson L. Albuquerque, [a] Gilberto Corso, [a] Eveline M. Bezerra, [a] Ewerton W. S. Caetano,[b] Roner F. da Costa [c] and Valder N. Freire[d]**

*Received Xth XXXXXXXXXX 20XX, Accepted Xth XXXXXXXXX 20XX*
*First published on the web Xth XXXXXXXXXX 200X*
**DOI: 10.1039/b000000x**

We employ quantum biochemistry methods based on the Density Functional Theory (DFT) approach to unveil detailed binding energy features of willardiines co-crystallized with the AMPA receptor. Our computational results demonstrate that the total binding energies of the fluorine-willardiine (FW), hydrogen-willardiine (HW), bromine-willardiine (BrW) and iodine-willardiine (IW) to the iGluR2 ligand-pocket correlate with the agonist binding energies, whose experimental sequence data match our computational counterpart, excluding the HW case. We obtain that the main contributions to the total willardiines-iGluR2 binding energy are due to the amino-acid residues in decreasing order Glu705 > Arg485 > Ser654 > Tyr450 > T655. Furthermore, Met708, which is positioned close to the 5-substituent, attracts HW and FW, but repels BrW and IW. Our results contribute significantly to an improved understanding of the willardiines-iGluR2 binding mechanisms.

## 1 Introduction

Disorders in the central nervous system (CNS) affect approximately 1 billion of the people around the world, leading to more hospitalizations than any other group of diseases [1]. Autism, schizophrenia, Alzheimer, Parkinson and epilepsy [2–6] have been ascribed to impairments on the ionotropic glutamate receptors (iGluRs) functions, which are ligand-gated ion channels that undergo structural changes after activation, culminating with the channel opening and generating an ion flux through the membrane [7]. The three major subclasses of iGluRs can be differentiated according to their amino-acids sequence and pharmacology as: kainate (GluK1-5), N-methyl-D-aspartic acid (NMDA; GluN1-3), and $\alpha$-amino-3-hydroxy-5-methyl-4-isoxazolepropionic acid (AMPA; GluR1-4) [8], being related to physiological processes such as memory and learning [9].

AMPA receptors have a key role in fast synaptic transmission [10], being well distributed throughout the CNS [11]. This type of receptor has a tetrameric structure organized as a dimer of dimers [12], where each monomer is composed of an extracellular amino-terminal region (ATD; approximately with 400 amino-acids), a ligand binding domain (LBD; approximately with 258 amino-acids) and a transmembrane region (TMD; approximately with 169 amino-acids) [13], whose molecular structures are depicted in Fig. 1. In it, each colour corresponds to a single chain and the circles in the LBD region represent the position of the ligand binding site in every subunit. The iGluR-LBD is formed by polypeptide segments (or lobes) $S1$ ($390-506$ amino-acids) and $S2$ ($632-775$ amino-acids) [14], which can be genetically combined and expressed as a soluble protein [15,16]. Its structural representation is shown in Fig. 2, which depicts the monomeric structure of the Ligand Binding Domain (LBD) coupled to a willardiine molecule (PDB ID: 1MQH). The letters N and C represent the amino and carboxyl terminal regions, respectively, that are linked to the Amino Terminal Domain (ATD) and the Transmembrane Domain (TMD) in the monomer. The circle marks the region of the protein investigated in this work. The amino-acids in this region are selected by increasing the binding region radius ($r$), see Table 1.

Crystallographic and electrophysiological studies have advanced significantly the structural and functional characterization of AMPA [17]. Isolated structures of LBD in complex with agonists, partial agonists and antagonists suggest a correlation between the degree of lobe closure and channel activation [18–22]. When bound to a full agonist, the lobes were closed by approximately 19.1 to 21.3 degrees, leading to channel activation with high efficacy levels [14,15,18]. In addition, antagonists have shown 2.5 to 9.6 degrees of lobe closure [14], blocking receptor activation. Finally, partial agonists induce an intermediate closure of the LBD (13.1 to 19 degrees) and the

[a] *Departamento de Biofísica e Farmacologia, Universidade Federal do Rio Grande do Norte, 59072-970, Natal-RN, Brazil. Fax: +-55-84-32153791; Tel: +-55-84-32153793; E-mail: umbertofulco@gmail.com*
[b] *Instituto Federal de Educação, Ciência e Tecnologia do Ceará, 60040-531, Fortaleza-CE, Brazil.*
[c] *Departamento de Física, Universidade Federal Rural do Semi-Árido, 59780-000 Caraúbas-RN, Brazil.*
[d] *Departamento de Física, Universidade Federal do Ceará, 60455-760, Fortaleza-CE, Brazil.*

| Ligand | r(Å) | | | | | | | | | | | | | | | | | | |
|---|---|---|---|---|---|---|---|---|---|---|---|---|---|---|---|---|---|---|---|
| | 2.0 | | | | 2.5 | | | | | 3.0 | | | | | | | 3.5 | | |
| FW | T480 | R485 | T655 | E705 | P478 | S654 | L704 | Y732 | – | Y450 | L479 | L650 | G653 | T686 | M708 | – | – | – | |
| HW | T480 | R485 | T655 | E705 | P478 | S654 | L704 | M708 | L650 | Y450 | L479 | G653 | T686 | Y732 | – | – | – | – | |
| BrW | T480 | R485 | T655 | E705 | P478 | S654 | L704 | Y732 | – | Y450 | L479 | G653 | T686 | – | – | – | L650 | M708 | |
| IW | T480 | R485 | E705 | – | P478 | S654 | T655 | L704 | Y732 | Y450 | L479 | G653 | M708 | – | – | – | L650 | T686 | |
| | 4.0 | | | 4.5 | | 5.0 | | | | | | 5.5 | | | | | | | |
| FW | E402 | K656 | – | S652 | L703 | I500 | T649 | Y702 | – | – | – | I400 | G451 | T482 | L498 | K730 | – | – | |
| HW | E402 | S652 | K656 | – | – | L498 | I500 | T649 | Y702 | L703 | – | I400 | G451 | T482 | K730 | – | – | – | |
| BrW | S652 | K656 | – | E402 | – | Y405 | L498 | I500 | T659 | Y702 | L703 | I400 | G451 | T482 | K730 | – | – | – | |
| IW | E402 | K656 | Y702 | Y405 | S652 | L498 | – | – | – | – | – | G451 | T482 | I500 | T649 | L703 | T707 | K730 | |
| | 6.0 | | | | | 6.5 | | | | | | | | 7.0 | | | | | |
| FW | Y405 | M463 | I481 | E657 | – | V464 | A477 | F491 | S501 | S706 | T707 | N709 | G731 | K449 | A452 | F658 | F659 | T685 | G733 | – |
| HW | Y405 | M463 | I481 | E657 | T707 | V464 | A477 | F491 | S501 | S706 | N709 | G731 | – | K449 | A452 | F658 | F659 | G733 | – | – |
| BrW | M463 | I481 | E657 | – | – | V464 | A477 | F491 | S501 | S706 | T707 | N709 | G731 | S403 | A452 | F658 | F659 | G733 | – | – |
| IW | I400 | M463 | I481 | E657 | – | S403 | A452 | A477 | F491 | S706 | G731 | – | – | P404 | K449 | V464 | S501 | F658 | N709 | G733 |
| | 7.5 | | | | 8.0 | | | | | | | | | | | | | | |
| FW | S403 | D651 | V683 | A687 | F495 | G499 | M503 | G648 | G689 | V690 | – | – | – | – | – | – | | | |
| HW | S403 | D651 | T685 | – | F495 | G499 | M503 | V683 | A687 | G689 | – | – | – | – | – | – | | | |
| BrW | P404 | K449 | D651 | R661 | F495 | G499 | M503 | G648 | V683 | T685 | A687 | G689 | V690 | Y711 | I712 | W767 | | | |
| IW | F659 | W767 | – | – | G448 | F495 | G499 | M503 | D651 | V683 | T685 | A687 | V690 | Y711 | I712 | – | | | |
| | 8.5 | | | | | | | | 9.0 | | | | | | | | | | |
| FW | L401 | P404 | G448 | W460 | G462 | I489 | R684 | I712 | V445 | N461 | A475 | V484 | M496 | I502 | F682 | Y711 | D728 | A735 | W767 |
| HW | L401 | G448 | W460 | G462 | I489 | G648 | V690 | I712 | P404 | N461 | V484 | M496 | I502 | F682 | R684 | Y711 | D728 | A735 | W767 |
| BrW | G448 | W460 | G462 | I489 | – | – | – | – | L401 | V445 | N461 | A475 | V484 | M496 | F682 | R684 | E710 | D728 | A735 |
| IW | W460 | G462 | I489 | M496 | G648 | G689 | – | – | L401 | C425 | V445 | N461 | A475 | V484 | R684 | E710 | D728 | – | – |
| | 9.5 | | | | | 10.0 | | | | | | | | | | | | | |
| FW | C445 | M674 | E688 | E710 | L727 | T399 | V406 | R453 | I476 | S497 | R660 | Y700 | | | | | | | |
| HW | V445 | A475 | E688 | E710 | L727 | T399 | V406 | C425 | R453 | I476 | S497 | M674 | | | | | | | |
| BrW | C445 | I502 | L727 | – | – | T399 | V406 | R453 | I476 | S497 | R660 | E688 | | | | | | | |
| IW | T399 | V406 | I502 | F682 | A735 | R453 | I476 | P494 | S497 | L727 | E688 | – | | | | | | | |
| | 10.5 | | | | | | | | | | | 11.0 | | | | | | | |
| FW | G465 | L467 | L483 | E486 | P494 | W671 | V693 | I734 | – | – | – | T398 | V681 | A701 | K722 | N726 | S729 | – | |
| HW | G465 | L467 | L483 | E486 | P494 | R660 | V693 | Y700 | K722 | I734 | – | T398 | W671 | A701 | – | – | – | – | |
| BrW | G465 | L467 | L483 | E486 | P494 | W671 | M674 | V693 | Y700 | K722 | I734 | T398 | Y424 | V681 | A701 | S729 | – | – | |
| IW | Y424 | G465 | L467 | L483 | E486 | R660 | W671 | K722 | I734 | K763 | – | T398 | M407 | D447 | M674 | V693 | Y700 | N726 | |
| | 11.5 | | | | | | | 12.0 | | | | | | | | | | | |
| FW | Y424 | D447 | R661 | M670 | A691 | R713 | – | M407 | L428 | V488 | Y647 | R692 | K763 | – | – | | | | |
| HW | Y424 | D447 | M670 | V681 | N726 | S729 | – | L428 | V488 | S492 | Y647 | R661 | A691 | E713 | K763 | | | | |
| BrW | M407 | D447 | M670 | A691 | E713 | N726 | K763 | L428 | V488 | S492 | Y647 | R692 | R715 | – | – | | | | |
| IW | R661 | V681 | A701 | E713 | S729 | K768 | – | L428 | V488 | S492 | M670 | A691 | R715 | – | – | | | | |

**Table 1** GluR2 residues interacting with fluorine-willardiine (FW), hydrogen-willardiine (HW), bromine-willardiine (BrW) and iodine-willardiine (IW) as the binding pocket radius *r* increases. The most important residues interacting with willardiines are shown in boldface. In red (blue) are the negatively (positively) charged residues, and in orange is the M708 residue.

opening of the ion channel.

The action of partial agonists in the production of submaximal responses has not yet been completely understood [16,23]. In this regard, a set of willardiines, from *Acacia willardiana* and *Mimosa asperata* [24–26], has been used to elucidate the molecular basis of partial agonism in AMPA [16,23,27,28].

Since 1980, willardiine and its analogues have been tested and proved to be a neurotransmitter composite [29–32]. The substitution of a single atom at the position 5 of the uracil ring of (s)-willardiine by *F*, *Cl*, *Br* and *I* has lead to different responses, suggesting their utilization in structure-function studies [33].

A comparison between the structures of glutamate coupled

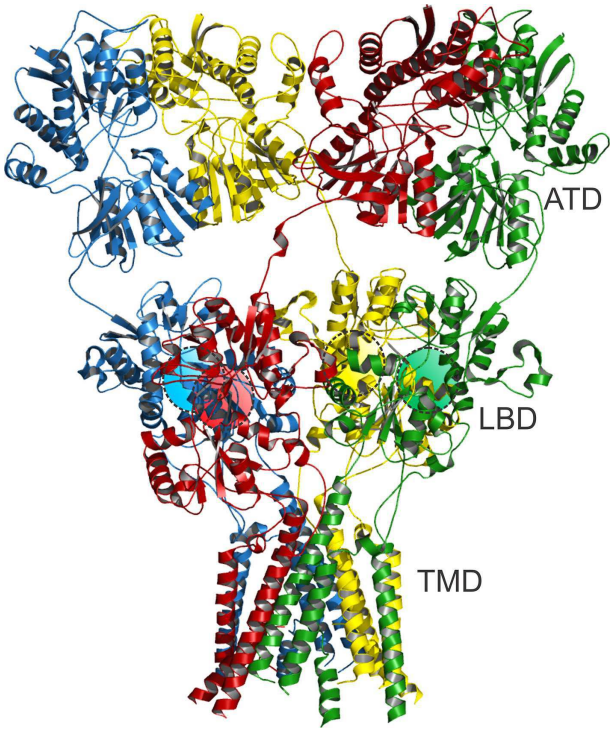


**Fig. 1** (color online) The Y-shaped GluR2 receptor structure and its monomers composed by the Amino-Terminal Domain (ATD), the Ligand-Binding Domain (LBD) and the Transmembrane Domain (TMD). Each colour corresponds to a single chain, and the circles in LBD region represent the position of the ligand binding site in every subunit. The PDB code is 3KG2 [13].

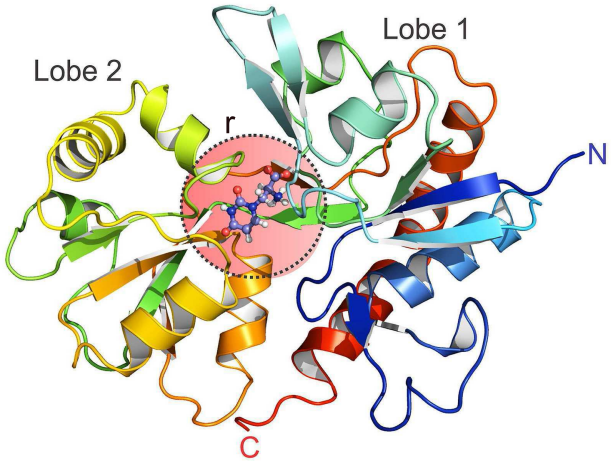


**Fig. 2** (color online) Structural representation of the Ligand-Binding Domaing (LBD) interface. The Binding Pocket Sphere (BPS) with radius (r) is also shown in this picture as a circle around the willardiine ligand. N and C represents the amino and carboxyl terminal regions.

to iGluRs-LDB with other full and partial agonists suggested that the groups $\alpha$-amino and $\alpha$-carboxyl occupy similar positions in the receptor [34]. This pattern was also observed during the superposition of the crystal structures of glutamate and four partial agonists willardiine, while the substituents attached at $\gamma$-position occupy different regions of the receptor [10,35].

Experimental, computational and crystallographic analysis has been used to describe partial agonism by 5-substituted willardiines in AMPA receptors [28,32,33,35,36]. The crystal structure of GluR2-LBD with four willardiines provided an opportunity to identify subtle structural differences on the receptor created by a single atom change in the ligand. The analysis of crystallographic structures can be done based on important tools like the distances and sizes of connections (*virtual screening*), the *de novo* design, molecular docking and molecular dynamics [37,38], these methods being limited by the lack of information on the interaction between specific residues of the receptor and the different ligands, which would be quite useful for the design of new drugs. Indeed, the use of quantum mechanics (QM) for *in silico* drug design has become quite popular in recent years due to its high accuracy in estimating relative binding affinities [39,40].

However, the high computational cost of QM methods to calculate the energies of interaction of macromolecules demands a balance between the computer execution time and the accuracy of the results. In view of this, fragmentation methods have been developed to make macromolecules computationally less expensive [41]. The molecular fractionation with conjugated caps (MFCC) method [42,43] has been widely used particularly to calculate the interaction energy between amino-acid fragments and ligands [44–46].

The aim of this work is to present an adequate description of the interaction of four willardine partial agonists with GluR2 through quantum biochemistry techniques within the Density Function Theory (DFT) framework. The individual contribution of each amino-acid residue was calculated applying the MFCC scheme [42,43] considering residues at the binding site, but also including other relevant residues. The simulations were performed using the X-ray structure of GluR2 co-crystallized with FW, HW, BrW and IW (PDB ID: 1MQI, 1MQJ, 1MQH and 1MQG respectively) [16]. A comparison between our theoretical binding energies and the experimental one is also made and their features discussed.

## 2 Materials and Methods

Crystallographic data of the willardiines FW, HW, BrW and IW co-crystalized with iGluR2 [16] were downloaded from the PDB database (http://www.rcsb.org) under the following codes (resolutions) 1MQI (1.35Å), 1MQJ (1.65Å), 1MQH (1.8Å) and 1MQG (2.15Å). The state of protonation of all

ligands at physiological pH was obtained using the Marvin Sketch code version 5.3.2 (Marvin Beans Suite - ChemAxon).

Hydrogen atoms, not resolved by the X-ray diffraction and therefore absent in the crystallographic files, were added to the structures and submitted to a classical geometry optimization fixing the other atoms. This optimization was performed using the classical force field CHARMm (*Chemistry at Harvard Molecular Mechanics*), which is especially parametrized for organic molecules[47].

Interaction energies for each residue at the binding site were performed using the DMol$^3$ code[48,49], within the Density Functional Theory (DFT) formalism. The Generalized Gradient Approximation (GGA) Perdew-Burke-Ernzerhof exchange-correlation functional(PBE)[50] and the Local Density Approximation (LDA) exchange-correlation functional according to the Perdew-Wang parameterization (PWC)[51] were chosen. It is true that the local density approximation is not the best option to achieve a good description of hydrogen bonds, but some DFT studies with this functional show good results for systems in which non-covalent interactions are relevant[52–54]. Moreover, recent works[37,38,44,45,55] have also shown satisfactory outcomes for calculations of interaction energies between amino-acids and ligands using a Double Numerical Plus polarization (DNP) basis set.

In order to improve the description of the non-covalent interactions, Ortmann *et al.*[56] and Grimme[57] have developed semiempirical approaches to provide a better compromise between the cost of first principles evaluation of the dispersion terms. Here, we used the DFT + D method following the GGA-PBE-Grimme and LDA-PWC-OBS (OBS is the Ortmann-Bechstedt-Schmidt correction[56]) schemes to calculate interaction energies of the four willardiine-GluR2 complexes. The DNP basis set, which, is comparable to the $6-311+G$ (3df, 2pd) basis set[48,49,58], was selected for the calculations to expand the Khon-Sham orbitals for all electrons. The orbital cutoff radius was set to $3.7\mathring{A}$, and the self-consistent field convergence threshold was adjusted to $10^{-6}$ Ha.

The interaction energy between each willardiine molecule and the amino-acid residues were calculated by using the formalism of the MFCC (Molecular Fractionation with Conjugate Caps) method[42,43]. The MFCC approach turns possible the investigation of a large number of amino-acid residues in a protein[37,38]. This technique of molecular fractionation lessens the computational time with no loss in accuracy[59,60].

A convergence study of the interaction energy as a function of the ligand binding pocket radius was performed to put a limit to the number of amino-acid residues to be analysed without missing important interactions,[38]. We investigated the variation of the total interaction energy considering the contributions of all amino-acid residues within a sphere of radius $r$, with origin in the ligand, capping the dangling bonds of each amino-acid residue[61]. Here we label the ligand molecule as $L$ and the $i-th$ amino-acid residue interacting with the ligand as $R^i$. The $C^{i-1}$ ($C^{i+1}$) cap is formed from the neighbour residues covalently bounded to the amine (carboxyl) group of the residue $R^i$ along the protein chain. As a matter of fact, for the willardine-iGluR2 systems here studied, the nearest five amino-acid fragments at each side of the $R^i$ residue were used to build the $C^{i-1}$ and $C^{i+1}$ caps, providing a better description of its electronic environment. For these fragmented structures, the interaction energy between the ligand and the individual fragments, $EI(L-R^i)$, is calculated according with:

$$\begin{aligned} EI(L-R^i) &= E(L+C^{1-i}R^iC^{i+1})-E(C^{1-i}R^iC^{i+1}) \\ &- E(L+C^{1-i}C^{i+1})+E(C^{1-i}C^{i+1}), \end{aligned} \quad (1)$$

where the first term $E(L+C^{i-1}R^iC^{i+1})$ is the total energy of the system formed by the ligand and the capped residue; the second term, $E(C^{i-1}R^iC^{i+1})$, is the total energy of the residue with the caps; the third term $E(L+C^{i-1}C^{i+1})$ is the total energy of the system formed by the caps and the ligand, and $E(C^{i-1}C^{i+1})$ is the energy of the caps with dangling bonds hydrogenated. The total interaction energy for each willardiine is obtained by adding up the interaction energies with each amino-acid residue within a given binding pocket radius. Water molecules were taken into account in the calculation procedures when hydrogen bonds are formed with the residues of interest or with the caps. A hydrogen bond length limit of $2.5\mathring{A}$ was adopted in this case.

## 3 Results and Discussions

Complexes with full agonists, partial agonists and antagonists are useful to relate structural and dynamic properties of the glutamate receptor S1S2 domain to functional properties that can be only measured for the intact protein. The series of willardiines considered in the present study are particularly suited for this analysis because they differ structurally at just one position, having functional properties that vary according to their electronegativity (potency and binding affinity) and size (efficacy and desensitization)[33].

The partial agonism of 5-substituted willardiines can help to understand the mechanisms of activation and desensitization of AMPA receptors. It was proposed that the size of the halogen substituent is directly involved in the modulation of the binding site and, consequently, in the closure of the lobes[10,16,28,35]. Results reported in Refs.[16,35,62], which relied on electrophysiological and crystallographic data, have been pivotal to grasp the partial agonism mechanism in iGluR2, showing that the potency increases with the electronegativity. Besides, the peak current and the extent of receptor desensitization varies according to the size of the substituent, which

implies that the extent of lobes closure affects the response of the receptor [16,23,28,35,62,63] .

Recently, Ahmed *et al.* [64] and Matinez *et al.* [65], have shown the importance of the willardiine protonation state in the activation of GluR2. To give a good explanation about the 5-substituted willardiine interactions with the AMPA receptor, we used the Marvin Sketch software to obtain their $pK_a$ curves at 7.3 pH value. In Fig. 3, we see the molar fraction curves in pH values between $0-12$ (Fig. 3a), and the molecular view of the two distinct protonation states of the four willardiine derivatives compounds (Fig. 3b). Our results shown that the uncharged protonation state has a larger contribution in comparison with the charged state, in agreement with Hill *et al.* [66] and Ahmed *et al.* [64]. For this reason, all calculations were made here with the N3 atom of the uracil ring in the uncharged state.

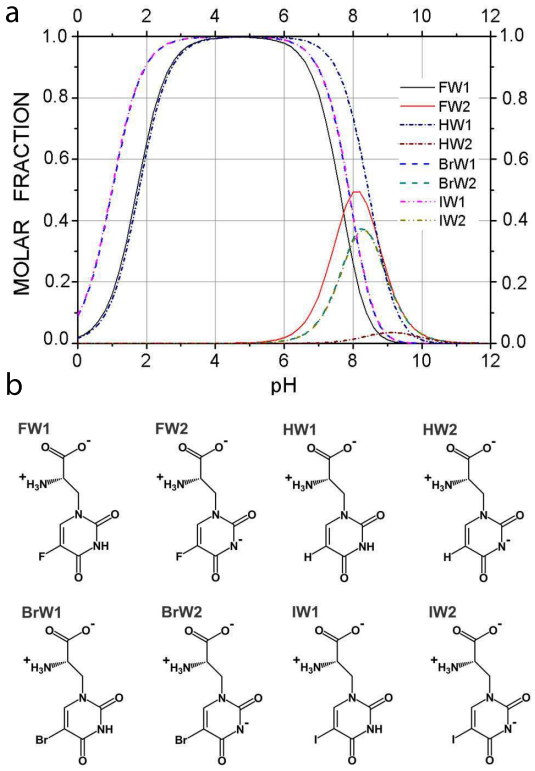


**Fig. 3** (color online) Protonation state of 5-substituted willardiines as a function of pH. (a) Molar fraction curves at pH $7.2-7.4$. (b) The two distinct molecular states for fluorine-willardiine (FW, solid lines), hydrogen-willardiine (HW, chain-dotted lines), bromine-willardiine (BW, dashed lines) and iodine-willardiine (IW, chain-doubled dotted lines) are depicted.

We analysed the binding pocket of the receptor employing the MFCC scheme to obtain the individual contribution of the amino-acid residues inside a binding pocket with a selected radius, ranking the most relevant interactions between residues and ligands. The total binding energy was obtained by adding up the individual contributions. To evaluate the binding interactions through fragment-based quantum mechanics method, it is important to take into account every significant attractive and repulsive amino-acid residue which can influence this mechanism. Therefore, instead of taking an arbitrary region of the binding site, we performed a search for an optimal binding pocket radius for which no significant variation in the total binding energy could be observed after a radius increase. For this task, the binding pocket radius $r$ was varied from $2.0\AA$ to $12\AA$ for all willardiines. In order to describe the most important ligand-residue interactions exhibited by GluR2 we have considered the compounds subdivided into two regions, as one can see in Fig. 4a. Fig. 4b depicts the electron density isosurface for $FW, HW, BrW$ and $IW$ series to observe how the electrons are distributed around the molecules and how their distribution is affected by the 5-substituted halogen atom. Differences in the electron density can be observed in the halogen substituent region.

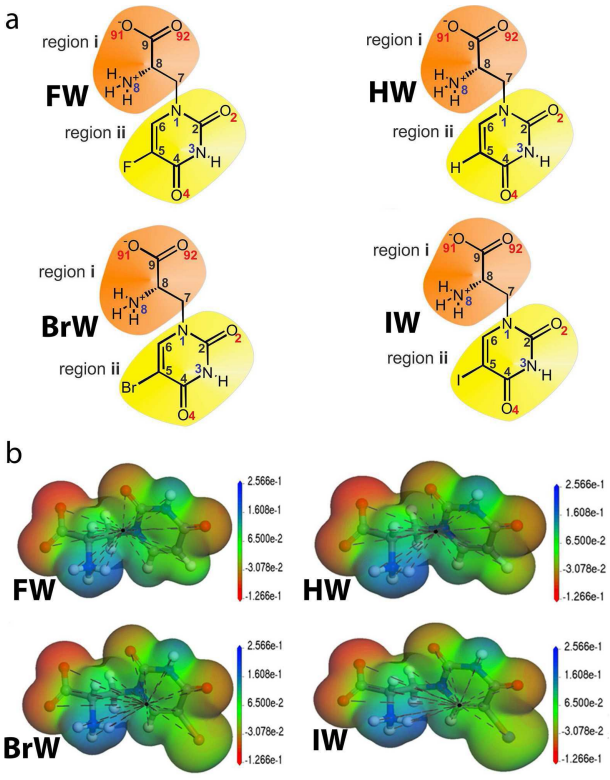


**Fig. 4** (color online) Willardiines FW, BrW, IW and HW: chemical representation at pH 7.3 and electron density distribution. (a) Region (**i**) contains the carboxyl and amine functional groups, while region (**ii**) corresponds to the uracil ring and its 5-substituents. (b) Electrostatic potencial surface and willardiine centroids.

Figures 5a and 5b show a comparison between the

calculated interaction energies $E(r)$ for the 5-substituted willardiines considering the binding pocket radius $r = 4.0, 6.0, 8.0, 10.0, 12.0\AA$. In Fig. 5a, using the GGA-PBE-Grimme approach, we found that at the smallest binding pocket radius ($4.0\AA$) the absolute value of the total 5-substituted willardiines interaction energy follows the order $HW > BrW > FW > IW$, which does not reproduce the corresponding experimental data[14]. For a binding pocket radius above $10.0\AA$, the absolute value of the binding energies E(r) follows the willardiine sequence $FW > HW > BrW > IW$. This result is close to the experimental sequence $FW > BrW > IW > HW$[16,33], meaning that the binding energy of each halogenated willardiine can be compared to its experimental value, the difference being in the position of the $HW$. The same occurs for the LDA-PWC-OBS case (see Fig. 5b), considering a smaller binding pocket radius ($4.0\AA$), although only above the $10.0\AA$ radius the total binding energy stabilizes as a function of $r$. One can note that, in this case, the LDA-PWC-OBS is very effective, confirming previously reported data[55].

The efficacy of the $HW$ and the three halogenated willardiine analogs $FW$, $BrW$, and $IW$, is correlated to the degree of closure of iGluR2-LBD lobes[16,33]. However, other mechanisms may influence the recognition and receptor activation, as the interaction between dimers. Besides, the dynamics of the AMPA receptor in complex with agonists, partial agonists and antagonists are not an easy task, as stressed by many authors. Among them, Postila *et al.*[32], although not addressing whether or not the closed lobe is required for activation of the channel, suggests that the closed lobe form is unstable for these partial agonists in agreement with many experimental works, being probably not required for the activation of the ion channel. Fenwick *et al.*[33] suggest that ligands with lower potency may be weakly bound to the protein, with the formation of multiple conformations to the ligand and amino-acids side-chain. Due to the mobility in the protein structure, there are many conformations obtained from the X-ray diffraction of the complex willardiine-GluR2. Thus, it is difficult to obtain the optimal conformation for our analysis, i.e., those that responds to the ligand binding affinity.

A detailed quantitative analysis to justify this conclusions is the following: the amino acids depicting a higher interaction energy with $HW$ are positioned in a similar way to that observed in $FW$. These amino acids interact with the atoms (C9)OO-, (N8)H, (C4)O4 and (N3)H with close proximity in $HW$, being responsible to a greater interaction energy not observed for $BrW$ and $IW$ since the size/electronegativity of the substituent halogen groups (Br and I) create a repulsion for some closed amino acids, such as M708 and C425. However, M708 and C425 have attractive energy for $FW$ and $HW$. Furthermore, contrary to what is observed for $FW$ and $HW$, amino acids that have a higher energy of interaction with $BrW$ and $IW$ are positioned close to the atoms (C2)O2, (N3)H and (C9)OO-. A full relation of the binding energy for all aminoacids is found in the provided supplementary material.

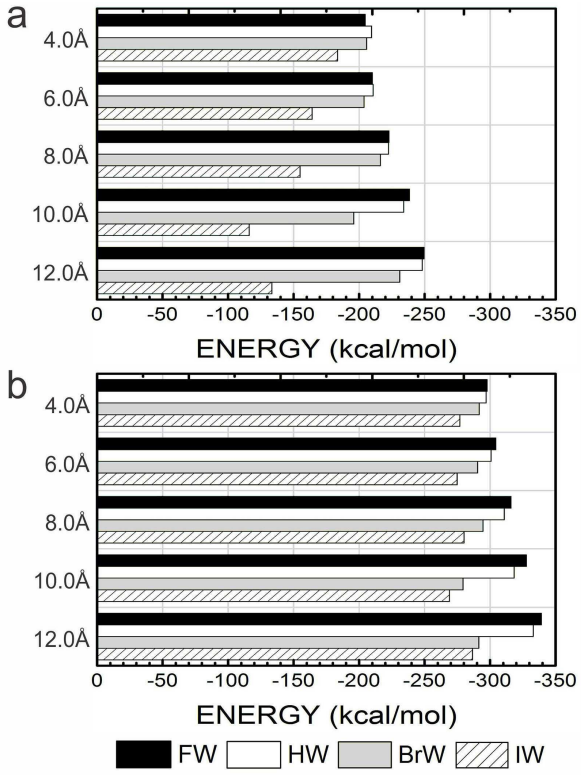


**Fig. 5** (color online) Total willardiine interaction energy for FW, HW, BrW and IW considering pocket radius values of $4.0\AA$, $6.0\AA$, $8.0\AA$, $10.0\AA$, and $12.0\AA$. (a) GGA-PBE-Grimme exchange-correlation functional results. (b) LDA-PWC-OBS exchange-correlation functional results. The absolute value of $E(r)$ obeys the sequence $FW > HW > BrW > IW$, reproducing the experimental data[16] excluding the $HW$ case.

Figure 6a-d shows a BIRD graphic panel (BIRD being an acronym of the keywords binding site, interaction energy and residues domain) with the interaction energies between the 5-substituted willardiine molecules and the most important amino-acid residues at the binding region. The panel depicts: (i) the interaction energy (in kcal/mol) of the residue with the ligands, illustrated by the horizontal bars, from which one can assign quantitatively the role of each residue in the binding site, i.e., their effectiveness as well as if they attract or repel the willardiines; (ii) the most important residues contributions to the bonding in the left side; (iii) the region (boldface letters, identified in Fig. 6) and the atoms of the ligands closer to each residue at the binding site. The binding energy of the amino-acid residues interacting with the willardiine molecule inside the binding pocket will be defined here as the negative of the corresponding interaction energy calculated using the MFCC

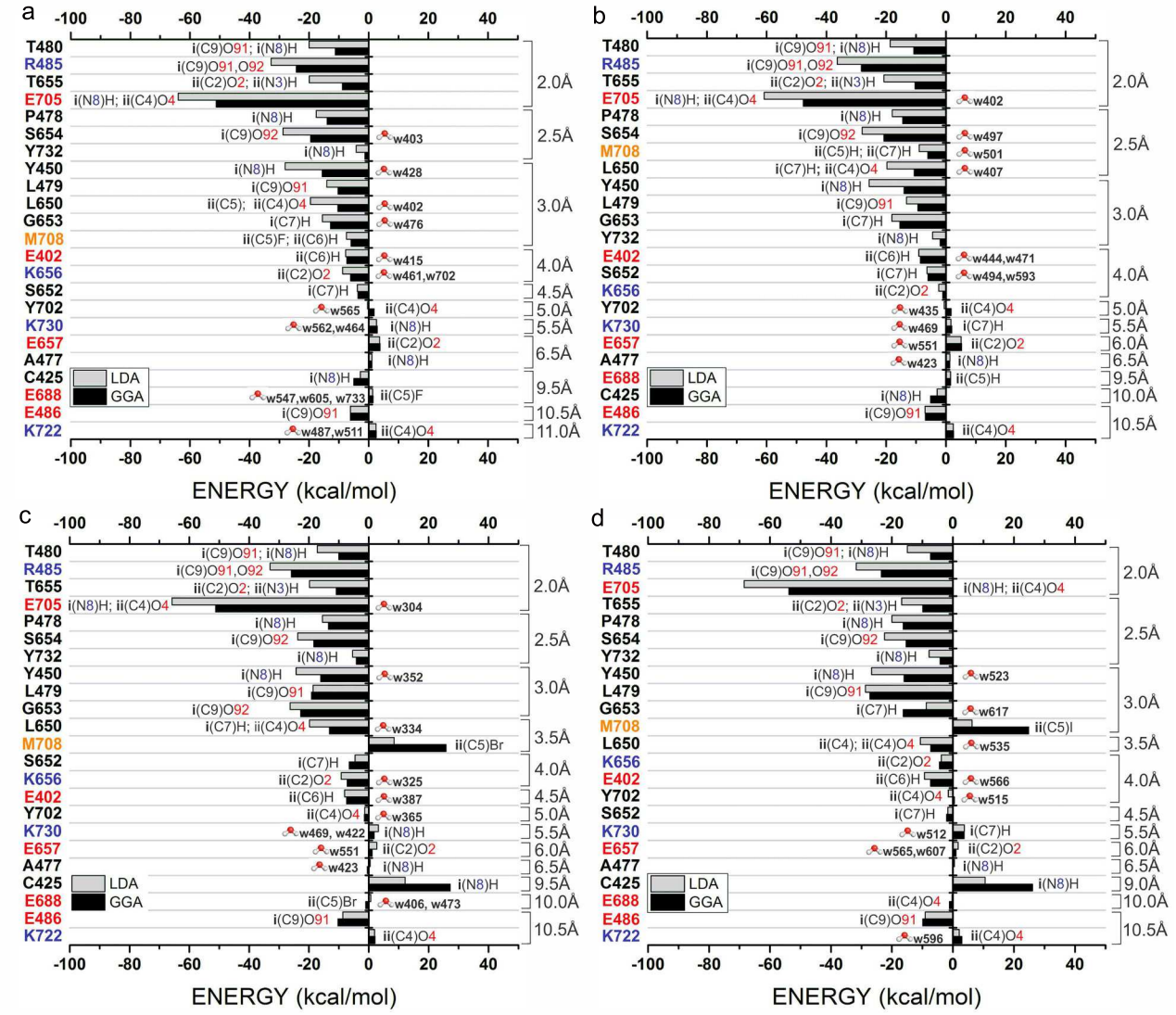


**Fig. 6** (color online) Binding site, interaction energy and residues domain (BIRD) graphic panel showing the most relevant residues of (a) FW, (b) HW, (c) BrW and (d) IW that contribute to the binding of each ligand.

method.

As one can see from Fig. 6, fourteen amino-acid residues are the most important for the stabilization of *FW*: T480, R485, T655, E705, P478, S654, Y450, L479, L650, G653, M708, E402, K656 and E486, while five amino-acid residues, K730, E657, A477, E688 and K722, display positive (repulsion) interaction energies. For *HW*, there are thirteen amino-acid residues helping the stabilization process: T480, R485, T655, E705, P478, S654, M708, Y450, L479, L650, G653, E402 and E486, while five amino-acid residues, K730, E657, A477, E688 and K722, work against the binding. For the case of *BrW*, there are thirteen amino-acid residues which are attractive: T480, R485, T655, E705, P478, S654, Y450, L479, G653, L650, K656, E402 and E486, while four amino-acid residues, M708, K730, E657 and K722, repel the ligand . Finally, for *IW* we have thirteen attractive amino-acid residues: T480, R485, E705, T655, P478, S654, Y450, L479, G653, L650, K656, E402 and E486, and four repelling amino-acid residues, M708, K730, E657 and K722.

Willardiines and glutamate bind to the ligand-binding core in a similar fashion [16]. Regions (**i**) and (**ii**) of willardiine (Fig. 4a) create a hydrogen bond network with R485, P478, T480 and S654, T655, E705 residues, like other agonists [15,35]. In order to display a systematically view of the interaction energies, the most important residues that contribute to the binding of the willardiines are represented in Table 2. This shown that

| Residue | Group | FW | | HW | | BrW | | IW | |
|---|---|---|---|---|---|---|---|---|---|
| | | d (Å) | $E_{GGA(LDA)}$ | d (Å) | $E_{GGA(LDA)}$ | d (Å) | $E_{GGA(LDA)}$ | d (Å) | $E_{GGA(LDA)}$ |
| **T480** | **i**(C9)O91; **i**(N8)H | 1.84; 1.96 | -11.21(-20.06) | 1.90; 2.15 | -10.73(-18.67) | 1.88; 2.11 | -10.03(-17.21) | 1.87; 2.17 | -7.38(-14.93) |
| **R485** | **i**(C9)O91, O92 | 1.75; 1.88 | -24.29(-32.79) | 1.81; 1.84 | -28.34(-36.44) | 1.68; 1.74 | -25.91(-32.97) | 1.71; 1.78 | -23.47(-31.72) |
| **T655** | **ii**(C2)O2; **ii**(N3)H | 1.95, 2.38; 1.90 | -8.80(-19.94) | 2.03, 2.43; 1.87 | -10.37(-20.78) | 2.03, 2.39; 1.91 | -10.92(-19.82) | 2.03; 2.14 | -9.88(-16.82) |
| **E705** | **i**(N8)H; **ii**(C4)O4 | 1.95; 1.99 | -51.21(-63.95) | 1.96; 1.97 | -47.77(-60.84) | 1.84; 2.00 | -51.24(-65.84) | 1.78; 2.15 | -53.80(-68.47) |
| **P478** | **i**(N8)H | 2.01 | -13.97(-17.61) | 2.02 | -14.51(-17.97) | 2.09 | -13.47(-15.47) | 2.00 | -16.29(-20.02) |
| **S654** | **i**(C9)O92 | 2.01 | -19.53(-28.77) | 2.06 | -20.74(-28.10) | 2.04 | -18.36(-23.79) | 2.02 | -15.37(-22.46) |
| **Y450** | **i**(N8)H | 2.82, 4.33 | -15.60(-28.08) | 2.89, 4.40 | -14.00(-25.71) | 3.00, 4.56 | -16.13(-24.32) | 3.00, 4.55 | -16.05(-26.76) |
| **L479** | **i**(C9)O91 | 2.71 | -10.28(-14.07) | 2.64 | -9.45(-13.25) | 2.63 | -19.16(-18.65) | 2.69, 2.69 | -27.27(-28.73) |
| **L650** | **ii**(C5); **ii**(C4)O4-FW<br>**i**(C7)H; **ii**(C4)O4-HW/BrW<br>**ii**(C4); **ii**(C4)O4-IW | 2.95; 4.09 | -10.36(-19.55) | 2.15; 4.15 | -10.64(-19.76) | 3.05; 4.27 | -13.13(-19.85) | 3.34; 5.75 | -7.29(-10.69) |
| **G653** | **i**(C7)H-FW/HW/IW<br>**i**(C9)O92-BrW | 2.60 | -12.83(-15.53) | 2.69 | -15.36(-18.08) | 2.66 | -22.78(-26.35) | 2.57 | -7.59(-8.73) |
| **M708** | **ii**(C6)H; **ii**(C5)F-FW<br>**i**(C7)H; **ii**(C5)H-HW<br>**ii**(C5)Br-BrW<br>**ii**(C5)I-IW | 2.53; 2.86 | -5.96(-7.52) | 2.53; 2.38 | -6.09(-8.93) | 3.09 | 25.80(8.45) | 2.76 | 24.82(6.28) |
| **E402** | **ii**(C6)H | 3.88 | -7.33(-7.73) | 3.76 | -8.55(-9.08) | 4.07 | -7.45(-8.08) | 4.00, 4.45 | -7.32(-9.35) |
| **K656** | **ii**(C2)O2 | 3.91, 4.14 | -6.07(-8.78) | 4.00 | -1.07(-2.44) | 3.99 | -7.23(-9.24) | 3.99 | -4.39(-3.79) |
| **Y702** | **ii**(C4)O4 | 4.61 | 1.76(-0.44) | 4.56 | 1.70(-0.59) | 4.63 | -1.51(-1.37) | 3.97, 4.33 | 0.45(-1.56) |
| **K730** | **i**(C7)H-FW/HW/IW<br>**i**(N8)H-BrW | 5.26 | 2.87(2.57) | 5.45 | 1.94(1.63) | 5.30, 5.77 | 1.77(3.17) | 5.39 | 3.63(3.70) |
| **E657** | **ii**(C2)O2 | 5.70 | 3.82(3.64) | 5.80 | 5.17(5.07) | 5.77 | 1.12(2.64) | 5.98 | 1.00(1.72) |
| **A477** | **i**(N8)H | 6.17 | 1.04(1.07) | 6.19 | 1.26(1.32) | 6.25 | -0.51(0.42) | 6.15 | -0.02(0.43) |
| **E688** | **ii**(C5)F-FW<br>**ii**(C5)H-HW<br>**ii**(C5)Br-BrW<br>**ii**(C4)O4-IW | 9.27 | 1.47(1.35) | 9.46 | 1.53(1.49) | 9.79 | -1.02(0.67) | 10.00 | -1.15(-0.27) |
| **E486** | **i**(C9)O91 | 10.29 | -6.16(-6.18) | 10.42 | -6.92(-6.99) | 10.32 | -10.29(-8.67) | 10.30 | -9.88(-9.08) |
| **K722** | **ii**(C4)O4 | 10.51 | 2.54(2.48) | 10.47 | 2.52(2.44) | 10.19 | 2.02(1.93) | 10.17 | 2.90(2.05) |

**Table 2** GGA (LDA) interaction energies and distances between the most important residues and 5-substituted willardiines at the binding pocket site of iGluR2. Red (blue) color stands for negatively (positively) charged residues and orange is the key residue Met708.

ten of the twenty amino-acids listed belong to region (**i**), and most of them show attractive interactions, with only two repulsive residues (K730 and A477). This is in accord with a previous study[36] which mentions region (**i**) as a recognition site of AMPA receptors. Region (**ii**), which is located at the $\gamma$-carboxyl position of glutamate, has seven important interacting residues with three of them repelling (E657, E688 and K722).

As observed in Fig. 7, E705 is the residue with the most intense binding energy contribution, attracting the ligand through a salt bridge between its side chain and the $\alpha$-amino group in region (**i**) (N8), and through a hydrogen bond in region (**ii**) (O4). After agonist binding, E705 undergoes a rearrangement that affects the domains closure[35]. Some works indicate that mutation or neutralization of E705 destabilizes LBD by decreasing the electrostatic repulsion between S1S2 domains[35,67–72]. Fig. 8 displays the electrostatic potential isosurfaces with projected electron densities for the willardines bound with the most important residues E705, S654, Y450, P478, and R485 at the binding pocket site.

The second highest energy contribution belongs to R485, whose side chain is facing the $\alpha$-carboxyl group of all four willardiines in region (**i**) and exhibits ionic and hydrogen bond interactions. The presence of R485 as a docking site to AMPA agonists is confirmed by molecular, theoretical and crystallographic studies[45,71,73]. S654 and T655 form H-bonds in regions (**i**) (O92) and (**ii**) (O2 and N3), respectively[16,33,45]. T655 forms only two hydrogen bonds, with *IW* having the

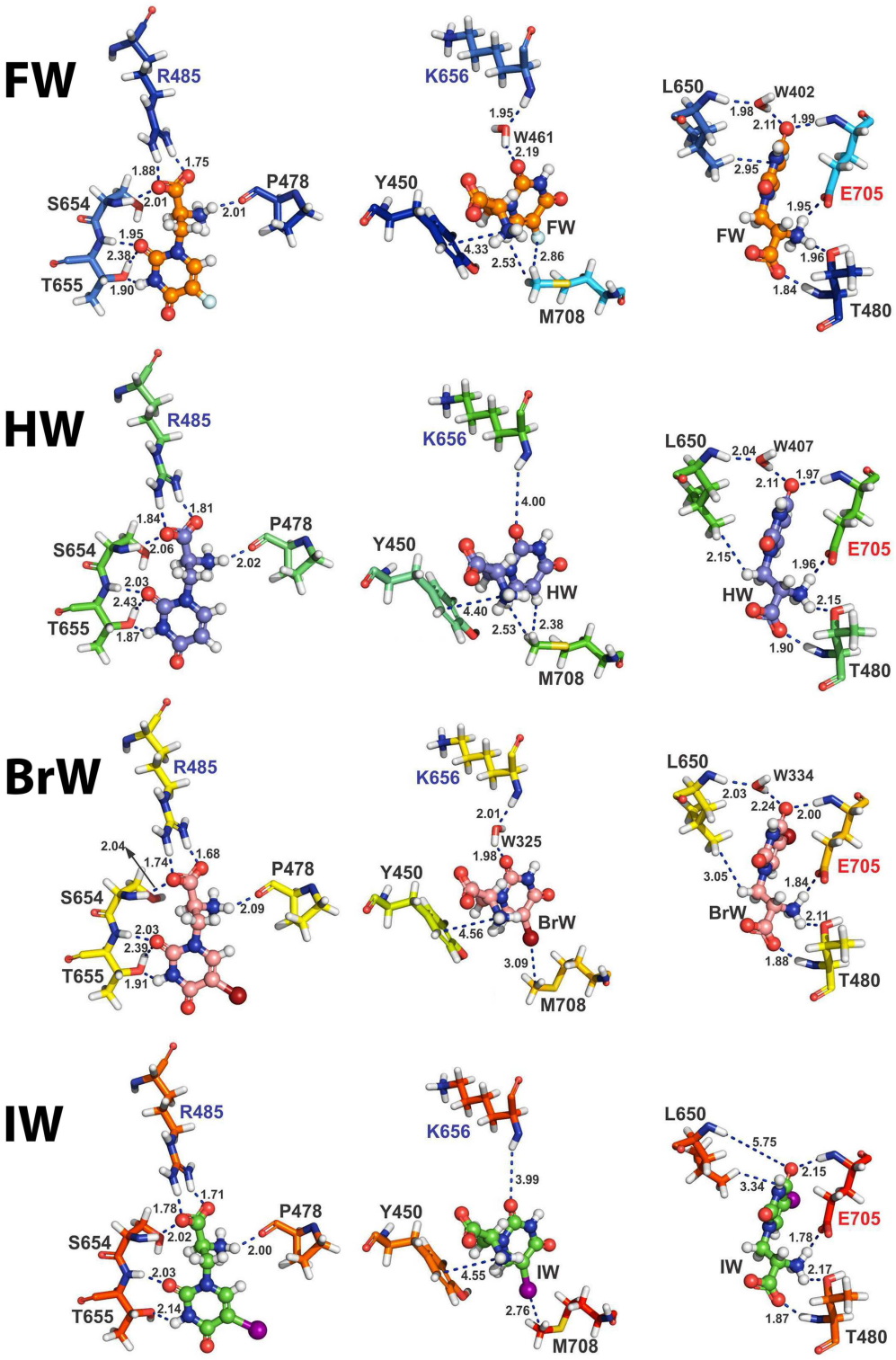


**Fig. 7** (color online) Distances between GluR2 residues and FW, HW, BrW, and IW. Their interaction energies are the most significant to the total binding energy of the 5-substituted willardiines.

lowest energy among other willardiines-T655 complexes (Fig. 6d). These three residues are positioned in close conformation to other complexes, stabilizing the $\alpha$-carboxyl (R485 and S654) and $\gamma$-carboxyl (T655) regions of the ligands[74].

Y450 form a cation-$\pi$ interaction in region (**i**) with the four willardiines. Holm *et al*[73] have reported that mutation Y450A results on a dramatic reduction in potency of glutamate to exclude the Y450 steric effect. As we can see, T480 interaction energy varies following the FW > HW > BrW > IW sequence, like S654, and forms two hydrogen bonds in region (**i**). Molecular dynamics shows that modifications in T480 increase significantly the D1-D2 repulsion[68], because the backbone amide stabilizes the $\alpha$-carboxyl group[75]. P478, along with T480, creates hydrogen bond with the $\alpha$-amino group of the willardiines.

K656 interacts with *FW* and *BrW* by water mediated hidrogen bonding (W461 and W325 molecules, respectively), with larger binding energy than K656-*HW* or *IW* complexes. Likewise, L650 shows the lowest energy when interacting with *IW*, being the only L650-willardiine complex without water mediated hydrogen bonds (see Fig. 7). It was pointed out that water molecules play a key role in modulating the cleft conformation[35]. This result is confirmed by our methodology if one considers the variation of calculated interaction energy values in residues with small distance shifts and water-mediated hydrogen bonds, such as L650 and K656.

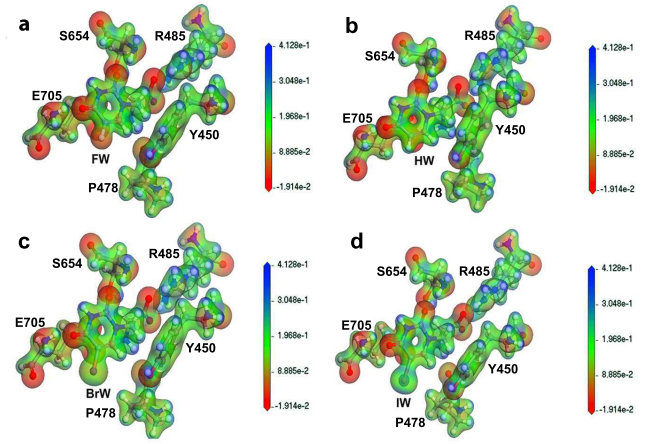


**Fig. 8** (color online) Electrostatic potential isosurfaces with the projected electron densities for 5-substituted willardiines, (a) FW , (b) HW , (c) BrW and (d) IW, interacting with the attractive residues E705, Sr654, Y450, P478 and R485.

Lastly, our analysis show that M708, which is positioned in the cavity surrounding the halogen substituent, interacts attractively with HW and FW, and repulsively with BrW and IW (see Table 1). This suggests that, together with the steric effect promoted by the size of the 5-substituted molecules, the closure of the individual domains might also be affected by the attractive/repulsive effect promoted by the electronegativity of the substituent atom. Thus, the increase in size of the 5-substituent and the repulsive effect of *Br* and *I* over Met708 can lead the ligand-binding core to adopt distinct conformations which reduce the domain closure and, consequently, shorten the intra-dimer separation in the ion channel gate. Among the 20 amino-acid residues analyzed in this work (see Table 2), E705 and R485 are the residues with larger contribution to the binding of 5-substituted willardiines interacting with the atom groups $i(N8)H; ii(C4)O4$ and $i(C9)O91, O92$ of the willardiines. The residues Y450, T480, and P478, among others, contribute with attractive interactions, while E657, K730 and K722 repel all 5-substituted willardiines. Moreover, it was suggested that Y450 has a key role in the orientation of glutamate through cation-$\pi$ interaction[71], while M708 seems to interact directly with the 5-substituent attracting HW and FW, and repelling BrW and IW.

## 4 Conclusions

One of the major goals in medicinal chemistry regarding drug discovery and design is to achieve an accurate description of the binding mechanism between the macromolecules of interest and their ligands. Quantum chemistry methods have proven to be a powerful tool to go in that direction, mainly due to the improvement of density functional theory (DFT) methods to describe intermolecular interactions[40].

The partial agonism of 5-substituted willardiines can be used to understand the mechanisms of activation and desensitization of AMPA receptors. It was proposed that the size of the halogen substituent is directly involved in the modulation of the binding site and, consequently, in the closure of the lobes and activation of the ionic channel[18–21]. As a matter of fact, results reported in Refs.[16,35] have been pivotal to the understanding of the partial agonist mechanism in iGluR2. However, it is not clear what is the protonation state of the 5-substituted willardiine responsible for the activation level observed in those works. Note that recently a reasonable number of papers have showed that partial agonists probably have different lobe orientations distributions, whose most stable crystal structures does not represent the entire mechanism of channel activation (Refs.[23,76–82] to cite just a few).

To fill this gap, we have performed DFT-dispersion corrected calculations using the GGA-PBE-Grimme and LDA-PWC-OBS exchange-correlation functionals to find out the interaction energy profile of a set of 5-substituted willardiines with GluR2. The main advantage of the methodology proposed here is the possibility to evaluate what amino-acid residues are more relevant to the stabilization of 5-substituted willardiines, which can be useful for drug design. A molecular fractionation scheme (MFCC) has allowed us to infer that

modifications in the region (**ii**), which define the specificity to willardiines ($\gamma$-position of Glu), are prone to create new potent agonists or antagonists[83].

In summary, we have investigated the interactions among 5-substituted willardiines and the extended GluR2 binding pocket using quantum chemistry calculations. We also demonstrate the necessity of taking into account a larger binding pocket size, including more distant amino-acid residues in order to obtain a good correlation between experimental and simulation data. After a convergence study on the size of the binding pocket sphere, we have taken into account all ligans-residue interactions within a radius of 12 *Å* from the ligand. Observe that *FW*, *BrW*, and *IW* have significant charged states at physiological pH. We tried to take this into account, but unfortunately we did not achieve a proper computer convergence of their total binding energies. Notwithstanding, it was already shown that uncharged protonation state is a possible representation of the molecule at physiological pH[64–66]. Our results suggest that the protonation state with uncharged uracil ring can represent the partial agonist effect on iGluR2 of the studied willardines. For willardiine-GluR2 complexes, the most important residues affecting the binding mechanism are: L650, E402, K656, T702 and E468. Significant energy contributions to the ligand binding also originate from other residues, following the sequence E705 $>$ R485 $>$ S654 $>$ Y450 $>$ T655 (in order of binding strength), as well as the interaction with M708.

## Acknowledgements

This work was partially financed by the Brazilian Research Agencies CAPES (Rede NanoBioTec, PNPD) and CNPq (INCT-Nano(Bio)Simes, Casadinho/Procad). E. W. S. C. received financial support from CNPq project 307843/2013-0.

## References

1 D. J. Wolak and R. G. Thorne, *Mol. Pharmaceutics*, 2013, **10**, 1492-1504.
2 R. Canitano and V. Scandurra, *Research in Autism Spectrum Disorders*, 2014, **8**, 255-265.
3 C. Jamieson, J. K. F. Maclean, C. I. Brown, R. A. Campbell, K. J. Gillen, J. Gillespie, B. Kazemier, M. Kiczun, Y. Lamont, A. J. Lyons, E. M. Moir, J. A. Morrow, J. Pantling, Z. Rankovic and L. Smith, *Bioorganic & Medicinal Chemistry Letters*, 2011, **21**, 805-811.
4 A. B. Nørholm, P. Francotte, L. Olsen, C. Krintel, K. Frydenvang, E. Goffin, S. Challal, L. Danober, I. Botez-Pop, P. Lestage, B. Pirotte and J. S. Kastrup, *J. Med. Chem.*, 2013, **56**, 8736-8745.
5 S. Ramaswamy, D. Cooper, N. Poddar, D. M. MacLean, A. Rambhadran, J. N. Taylor, H. Uhm, C. F. Landes and V. Jayaraman, *J. Biol. Chem.*, 2012, **287**, 43557-43564.
6 P. Stawski, H. Janovjak and D. Trauner, *Bioorganic & Medicinal Chemistry*, 2010, **18**, 7759-7772.
7 K. Poon, L. M. Nowak and R. E. Oswald, *Biophysical Journal*, 2010, **99**, 1437-1446.
8 D. Lodge, *Neuropharmacology*, 2009, **56**, 6-21.
9 E. Gouaux, *J. Physiol.*, 2003, **554.2**, 249-253.
10 M. L. Mayer, *Nature*, 2006, **440**, 456-462.
11 D. C. Javitt, *Molecular Psychiatry*, 2004, **9**, 984-997.
12 D. R. Madden, *Nature Reviews*, 2002, **3**, 91-101.
13 A. I. Sobolevsky, M. P. Rosconi and E. Gouaux, *Nature*, 2009, **462**, 745-756.
14 J. Pøhlsgaard, K. Frydenvang, U. Madsen and J.S. Kastrup, *Neuropharmacology*, 2011, **60**, 135-150.
15 N. Armstrong and E. Gouaux, *Neuron*, 2000, **28**, 165-181.
16 R. Jin, T. G. Banke, M. L. Mayer, S. F. Traynelis and E. Gouaux, *Nat. Neurosci.*, 2003, **6**, 803-810.
17 S. F. Traynelis, L. P. Wollmuth, C. J. McBain, F. S. Menniti, K. M. Vance, K. K. Ogden, K. B. Hansen, H. Yuan, S. J. Myers and R. Dingledine, *Pharmacol. Rev.*, 2010, **62**, 405-496.
18 A. Y. Lau, and B. Roux, *Nat. Struct. Mol. Biol.*, 2011, **18**, 283-287.
19 N. Armstrong, Y. Sun, C. Q. Chen, and E. Gouaux, *Nature*, 1998, **395**, 913-917.
20 N. Armstrong, M. Mayer and E. Gouaux, *Proc. Natl. Acad. Sci. U.S.A*, 2003, **100**, 5736-5741.
21 W. Zhang, Y. Cho, E. Lolis and J. R. Howe, *J. Neurosci.*, 2008, **28**, 932-943.
22 H. Dong and H. X. Zhou, *Nat. Commun.*, 2011, **2**, 354.
23 K. Poon, A. H. Ahmed, L. M. Nowak and R. E. Oswald, *Mol. Pharmacol.*, 2011, **80**, 49-59.
24 R. Gmelin, *Hoppe Seylers Z Physiol Chem.*, 1959, **316**, 164-169.
25 R. Gmelin, *Acta Chem. Scand.*, 1961, **15**, 1188-1189.
26 G. J. Krauss and H. Reinbothe, *Phytochemistry*, 1973, **12**, 125-142.
27 D. Patneau, M. Mayer, D. Jane and J. Watkins, *J. Neurosci.*, 1992, **12**, 595-606.
28 P. Kizelsztein, M. Eisenstein, N. Strutz, M. Hollmann and V. I. Teichberg, *Biochemistry*, 2000, **39**, 12819-12827.
29 R. H. Evans, A.W. Jones and J. C. Watkins, *J. Physiol.*, 1980, **308**, 71P-72P.
30 S. G. Agrawal and R. H. Evans, *Br. J. Pharmacol.*, 1986, **87**, 345-355.
31 C. F. Zorumski, L. L. Thio and D. B. Clifford, *Mol. Pharmacol.*, 1991, **40**, 45-51.
32 P. A. Postila, M. Ylilauri and O. T. Pentikäinen, *J. Chem. Inf. Model.*, 2011, **51**, 1037-1047.
33 M. K. Fenwick and R. E. Oswald, *J. Mol. Biol.*, 2008, **378**, 673-685.
34 M. L. Mayer and N. Armstrong, *Annu. Rev. Physiol.*, 2004, **66**, 161-181.
35 R. Jin and E. Gouaux, *Biochemistry*, 2003, **42**, 5201-5213.
36 A. S. Maltsev, A. H. Ahmed, M. K. Fenwick, D. E. Jane and R. E. Oswald, *Biochemistry*, 2008, **47**, 10600-10610.
37 I. L. Barroso-Neto, J. P. C. Marques, R. F. da Costa, E. W. S. Caetano, B. S. Cavada, C. Gottfried, and V. N. Freire, *J. Phys. Chem. B*, 2012, **116**, 3270-3279.
38 R. F. da Costa, V. N. Freire, E. M. Bezerra, B. S. Cavada, E. W. S. Caetano, J. L. de Lima Filho and E. L. Albuquerque, *Phys. Chem. Chem. Phys.*, 2012, **14**, 1389-1398.
39 T. Zhou, D. Huang and A.Caflisch, *Current Topics in Medicinal Chemistry*, 2010, **10**, 33-45.
40 K. Raha, M. B. Peters, B. Wang, N. Yu, A. M. Wollacott, L. M. Westerhoff and K. M. Merz, *Drug Discovery Today*, 2007, **12**, 725-731.
41 M. S. Gordon, D. G. Fedorov, S. R. Pruitt and L. V. Slipchenko, *Chem. Rev.*, 2012, **112**, 632-672.
42 D. W. Zhang and J. Z. H. Zhang, *J. Chem. Phys.*, 2003, **119**, 3599-3605.
43 D. W. Zhang, X. H. Chen and J. Z. H. Zhang, *J. Comput. Chem.*, 2003, **24**, 1846-1852.
44 G. Zanatta, I. L. Barroso-Neto, V. Bambini-Junior, M. F. Dutra, E. M. Bezerra, R. F. da Costa, E. W. S. Caetano, B. S. Cavada, V. N. Freire and C. Gottfried, *J. Proteomics & Bioinformatics*, 2012, **5**, 155-162.
45 A. C. V. Martins, P. Lima-Neto, I. L. Barroso-Neto, B. S. Cavada, V. N.

Freire and E. W. S. Caetano, *RSC Advances*, 2013, **3**, 14988-14992.
46 X. H. Chen and J. Z. H. Zhang, *J. Chem. Phys.*, 2004, **120**, 11386-11391.
47 F. A. Momany and R. Rone, *J. Comp. Chem.*, 1992, **13**, 888-900.
48 B. Delley, *J. Chem. Phys.*, 1990, **92**, 508-517.
49 B. Delley, *J. Chem. Phys.*, 2000, **113**, 7756-7764.
50 J. P. Perdew, K. Burke and M. Ernzerhof, *Phys. Rev. Lett.*, 1996, **77**, 3865-3868.
51 J. P. Perdew and Y. Wang, *Phys. Rev. B*, 1992, **45**, 13244-13249.
52 E. A. Kee, M. C. Livengood, E. E. Carter, M. McKenna and M. Cafiero, *J. Phys. Chem. B*, 2009, **113**, 14810-14815.
53 F. Ortmann, K. Hannewald and F. Bechstedt, *J. Phys. Chem. B*, 2008, **112**, 1540-1548.
54 F. Ortmann, W. G. Schmidt and F. Bechstedt, *Phys. Rev. Lett.*, 2005, **95**, 186101(4).
55 T. C. S. Ribeiro, R. F. da Costa, E. M. Bezerra, V. N. Freire, M. L. Lyra and V. ManzoniI, *New J. Chem.*, 2014, **38**, 2946-2957.
56 F. Ortmann, F. Bechstedt and W. G. Schmidt, *Phys. Rev. B*, 2006, **73**, 205101(10).
57 S. Grimme, *J. Comput. Chem.*, 2006, **27**, 1787-1799.
58 Y. Inada and H. Orita, *J. Comput. Chem.*, 2008, **29**, 225-232.
59 A. M. Gao, D. W. Zhang, J. Z. H. Zhang and Y. Zhang, *Chem. Phys. Lett.*, 2004, **394**, 293-297.
60 X. Chen, Y. Zhang and J. Z. H. Zhang, *J. Chem. Phys.*, 2005, **122**, 184105.
61 E. L. Wu, Y. Mei, K. L. Han and J. Z. H. Zhang, *Biophys. J.*, 2007, **92**, 4244-4253.
62 A. Frandsen, D. S. Pickering, B. Vestergaard, C. Kasper, B. B. Nielsen, J. R. Greenwood, G. Campiani, C. Fattorusso, M. Gajhede, A. Schousboe and J. S. Kastrup, *Mol. Pharmacol.*, 2005, **67**, 703-713.
63 L. A. Wong, M. L. Mayer, D. E. Jane and J. C. Watkins, *J. Neurosci.*, 1994, **14**, 3881-3897.
64 A. H. Ahmed, C. P. Ptak, M. K. Fenwick, C. L. Hsieh, G. A. Weiland and R. E. Oswald, *J. Bio. Chem*, 2013, **288**, 27658-27666.
65 M. Martinez, A. H. Ahmed, A. P. Loh and R. E. Oswald, *Biochemistry*, 2014, **53**, 3790-3795.
66 R. A. Hill, L. J. Wallace, D. D. Miller, D. M. Weinstein, G.. Shams, H. Tai, R. T. Layer, D. Willins, N. J. Uretsky and S. N. Danthi, *J. Med. Chem*, 1997, **40**, 3182-3191.
67 K. Speranskiy and M. Kurnikova, *Biochemistry*, 2005, **44**, 11508-11517.
68 T. Mamonova, M. J. Yonkunas and M. G. Kurnikova, *Biochemistry*, 2008, **47**, 11077-11085.
69 M. Kubo, E. Shiomitsu, K. Odai, T. Sugimoto, H. Suzuki and E. Ito, *J. Mol. Struct. (Theochem)*, 2003, **639**, 117-128.
70 A. Hogner, J. R. Greenwood, T. Liljefors, M. L. Lunn, J. Egebjerg, I. K. Larsen, E. Gouaux and J. S. Kastrup, *J. Med. Chem.*, 2003, **46**, 214-221.
71 O. Okada, K. Odai, T. Sugimoto and E. Ito, *Biophys. Chem.*, 2012, **162**, 35-44.
72 J. Boström, A. Hogner, S. Schimitt, *J. Med. Chem.*, 2006, **49**, 6716-6725.
73 M. M. Holm, P. Naur, B. Vestergaard, M. T. Geballe, M. Gajhede, J. S. Kastrup, S. F. Traynelis and J. Egebjerg, *J. Bio. Chem.*, 2005, **280**, 35469-35476.
74 R. L. McFeeters and R. E. Oswald, *Biochemistry*, 2002, **41**, 10472-10481.
75 A. H. Ahmed, M. D. Thompson, M. K. Fenwick, B. Romero, A. P. Loh, D. E. Jane, H. Sondermann and R. E. Oswald, *Biochemistry*, 2009, **48**, 3894-3903.
76 Q. Cheng and V. Jayaraman, *J. Biol. Chem.*, 2004, **279**, 26346-26350.
77 M.S. Horning and M.L. Mayer, *Neuron*, 2004, **41**, 379-388.
78 M.L. Mayer, *Curr. Opin. Neurobiol.*, 2011, **21**, 1-8.
79 A.H. Ahmed, S. Wang, H.H. Chuang and R.E. Oswald, *J. Biol. Chem.*, 2011, **286**, 35257-35266.
80 M. Kubo and E. Ito, *Proteins*, 2004, **56**, 411-419.
81 D.R. Madden, Q. Cheng, S. Thiran, S. Rajan, F. Rigo, K. Keinänen, S. Reinelt, H. Zimmermann and V. Jayaraman, *Biochemistry*, 2004, **43**, 15838-15844.
82 K.A. Mankiewicz, A. Rambhadran, L. Wathen and V. Jayaraman, *Biochemistry*, 2008, **47**, 398-404.
83 J. C. A. More, H. M. Troop, N. P. Dolman and D. E. Jane, *Br. J. Pharmacol.*, 2003, **138**, 1093-1100.